

# Preparation and characterization of the strontium stannates $\text{SrSnO}_3$ and $\text{Sr}_2\text{SnO}_4$

G. PFAFF

Merck KGaA, Research and Development, Pigment Division,  
P. O. Box, 64271 Darmstadt, Germany  
E-mail: gerhard.pfaff@merck.de

The strontium stannates  $\text{SrSnO}_3$  and  $\text{Sr}_2\text{SnO}_4$  can be synthesized by the wet chemical peroxide route. The first step of the preparation is the precipitation of stoichiometric peroxy precursors which can be transformed into the corresponding stannates by thermal degradation. The resulting very fine, single-phase strontium stannate powders have extremely small impurity contents. They show a very fast densification behaviour during sintering at temperatures above 1200 °C. A phase  $\text{Sr}_3\text{Sn}_2\text{O}_7$  could not be prepared using the peroxide route. © 2000 Kluwer Academic Publishers

## 1. Introduction

Alkaline earth stannates have received more and more attention in recent years as components of ceramic dielectric elements [1]. Strontium stannate,  $\text{SrSnO}_3$ , has been reported to be used in humidity sensors [2]. Solid solutions of alkaline earth titanates and stannates are also used for the fabrication of ceramic boundary layer capacitors [3]. The phase equilibria in the SrO– $\text{SnO}_2$  system have been studied by several authors [4–6]. The existence of the two stable phases  $\text{SrSnO}_3$  and  $\text{Sr}_2\text{SnO}_4$  has been reported [4, 5]. A phase of the composition  $\text{Sr}_3\text{Sn}_2\text{O}_7$  was identified in the binary system SrO– $\text{SnO}_2$  at 1350 °C [6].

$\text{SrSnO}_3$ , the most important of these compositions, is a dielectric material of technological importance. It is normally synthesized at temperatures above 1000 °C by solid-state reaction between  $\text{SrCO}_3$  or SrO and  $\text{SnO}_2$ . It crystallizes in the cubic system of perovskite [5, 7]. The relatively high preparation temperatures lead often to powders of large and varied grain sizes and varying impurity content.

$\text{Sr}_2\text{SnO}_4$  is found to be stable in the tetragonal  $\text{K}_2\text{NiF}_4$  structure [6, 8]. There exist two continuous series of solid solutions with  $\text{Ba}_2\text{SnO}_4$  and  $\text{Sr}_2\text{TiO}_4$  [6]. The formation of  $\text{Sr}_2\text{SnO}_4$  occurs at temperatures between 1000 °C and 1250 °C starting from  $\text{SrCO}_3$  and  $\text{SnO}_2$  [5, 6].  $\text{Sr}_3\text{Sn}_2\text{O}_7$  crystallizes in a rhombic structure [6]. There is a limited series of solid solutions with  $\text{Sr}_3\text{Ti}_2\text{O}_7$ . A maximum of 5% Sn can be substituted by Ti. On the other hand, there exists a continuous series of solid solutions with  $\text{Ba}_3\text{Sn}_2\text{O}_7$  [6].

There is only few information on the wet chemical possibility of preparing  $\text{SrSnO}_3$  fine powders [1]. So it is possible to synthesize this material in a powdered form via the precipitated hydrated stannate of the formal composition  $\text{SrSnO}_3 \cdot 3\text{H}_2\text{O}$ . The evaporation of water during calcination occurs below 300 °C, and the first  $\text{SrSnO}_3$  reflections in the X-ray diffractogram can be indicated at temperatures of about 430 °C [1].

An alternative way for the preparation of high purity barium, magnesium and calcium stannates is the peroxide route [9–11]. Various strontium, barium, magnesium and calcium titanates can also be synthesized using this method [12–15]. The peroxy precursor  $\text{BaZrO}_2(\text{O}_2) \cdot 6\text{H}_2\text{O}$  can be used for the synthesis of  $\text{BaZrO}_3$  [16]. Generally, peroxy precursors are formed by a precipitation reaction and decomposed by thermal treatment to the corresponding stannates, titanates or zirconates [9–16].

In the present work, experiments were carried out to investigate the formation of  $\text{SrSnO}_3$  and  $\text{Sr}_2\text{SnO}_4$  using the peroxide route. Investigations for the synthesis of the composition  $\text{Sr}_3\text{Sn}_2\text{O}_7$  are also described. The precipitation of the strontium- and tin-containing precursors, their thermal degradation to the stannates and the characterization of intermediate products and the final stannate powders as well as the results from sintering studies are presented here. The results are compared with those obtained for barium, magnesium and calcium stannates formed using the peroxide route.

## 2. Experimental procedure

A starting solution was prepared by dissolving  $\text{SrCl}_2 \cdot 6\text{H}_2\text{O}$  (Merck KGaA, Darmstadt) and  $\text{SnCl}_4$  (Merck KGaA, Darmstadt) in dilute hydrochloric acid. The Sn concentration used was 0.6 mol l<sup>-1</sup>. This solution was added rapidly at 10 °C under argon in a 1.5-fold volume of a solution of hydrogen peroxide and ammonia in water. The molar ratios of  $\text{SrCl}_2 \cdot 6\text{H}_2\text{O}$  to  $\text{SnCl}_4$  to  $\text{H}_2\text{O}_2$  to  $\text{NH}_3$  used were 1 : 1 : 2.5 : 12 for  $\text{SrSnO}_3$ , 2 : 1 : 5 : 12 for  $\text{Sr}_2\text{SnO}_4$  and 3 : 2 : 7 : 20 for  $\text{Sr}_3\text{Sn}_2\text{O}_7$ . Light yellow amorphous precipitates were formed in all cases during the addition of the strontium- and tin-containing solutions. The precipitates were filtered and washed with deionized water. No chloride was found after washing. The wet powders were then dried with concentrated sulphuric acid in a desiccator. They were

calcined at different temperatures up to 1000 °C to form stannate phases.

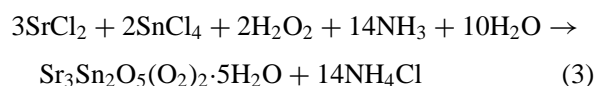
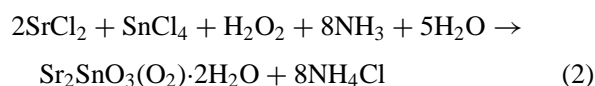
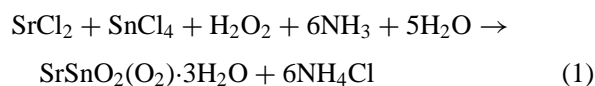
The as-prepared precursors and heat-treated powders were investigated by chemical analysis as follows: tin was analyzed gravimetrically as SnO<sub>2</sub>, and strontium was titrated complexometrically with thymolphthalein as indicator. The peroxide content of the precipitates was analyzed iodometrically.

Thermal decomposition of the peroxo-precursors was investigated by thermo-gravimetry (Thermogravimetric Analyzer 951 system, DuPont Instruments, heating rate 600 °C h<sup>-1</sup>) and differential thermal analysis (Thermal Analyst System 2100, DuPont Instruments, heating rate 300 °C h<sup>-1</sup>). An air atmosphere was used for these measurements. X-ray diffraction investigations (Philips PW 1710 diffractometer, Ni filter and Cu K<sub>α</sub> radiation) allowed the formation of the stannate phases to be located. Certain impurities were measured using atomic absorption spectrometry (Perkin-Elmer 303) and atomic emission spectrometry (PGS 2 apparatus, Carl Zeiss Jena). Surface characterization was carried out by BET measurements (Accusorb 2100 D, Micromeritics, nitrogen adsorption).

The strontium stannates SrSnO<sub>3</sub> and Sr<sub>2</sub>SnO<sub>4</sub> obtained as powders by calcining the precursors at 1000 °C for 1 h were investigated with respect to their sintering behaviour. The powders were mixed with a binder solution (65% H<sub>2</sub>O, 25% glycerol, 10% polyvinyl alcohol) in a mortar, deagglomerated for 20 min in a vibratory mill, dried and sieved out at 80 mesh. The resulting powders were pressed in the form of discs under a pressure of 125 MPa and sintered at 1200 °C and 1400 °C. The densities of the pellets were determined by weighing and measuring the dimensions using a micrometer before and after each heating step.

### 3. Results and discussion

The analytical results of the dried precursors and of the powders obtained after calcination at 1000 °C are summarized in Table I. The values for the strontium, tin and peroxide contents are very close to the expected stoichiometric compositions. SrSnO<sub>2</sub>(O<sub>2</sub>)·3H<sub>2</sub>O, Sr<sub>2</sub>SnO<sub>3</sub>(O<sub>2</sub>)·2H<sub>2</sub>O, and Sr<sub>3</sub>Sn<sub>2</sub>O<sub>5</sub>(O<sub>2</sub>)<sub>2</sub>·5H<sub>2</sub>O are the formal compositions for the three precursors. The reactions for the precursor formation can be summarized by the following equations:



The used preparation route results in light yellow homogeneous powders which, on thermal treatment up to temperatures above 500 °C, lead to crystalline materials. A similar situation has been found for the corresponding barium, magnesium and cal-

TABLE I Analytical data for the peroxo precursors and for the products obtained after thermal treatment at 1000 °C (weight loss for 1 h at 1000 °C)

Component	SrSnO <sub>2</sub> (O <sub>2</sub> )·3H <sub>2</sub> O		SrSnO <sub>3</sub>	
	Exp. (%)	Calc. (%)	Exp. (%)	Calc. (%)
Strontium	26.9	27.0	34.4	34.4
Tin	36.5	36.6	46.8	46.7
Peroxide	9.7	9.9	—	—
Weight loss	22.0	21.6	—	—
Component	Sr <sub>2</sub> SnO <sub>3</sub> (O <sub>2</sub> )·2H <sub>2</sub> O		Sr <sub>2</sub> SnO <sub>4</sub>	
	Exp. (%)	Calc. (%)	Exp. (%)	Calc. (%)
Strontium	42.7	42.7	48.9	49.0
Tin	29.1	29.0	33.3	33.2
Peroxide	7.5	7.8	—	—
Weight loss	13.0	12.7	—	—
Component	Sr <sub>3</sub> Sn <sub>2</sub> O <sub>5</sub> (O <sub>2</sub> ) <sub>2</sub> ·5H <sub>2</sub> O		"Sr <sub>3</sub> Sn <sub>2</sub> O <sub>7</sub> "	
	Exp. (%)	Calc. (%)	Exp. (%)	Calc. (%)
Strontium	35.8	35.8	42.8	42.9
Tin	32.2	32.3	38.7	38.8
Peroxide	8.6	8.7	—	—
Weight loss	16.9	16.6	—	—

cium stannate precursors. These have the compositions BaSnO<sub>2</sub>(O<sub>2</sub>)<sub>2</sub>·3H<sub>2</sub>O, Ba<sub>2</sub>SnO<sub>3</sub>(O<sub>2</sub>)·2H<sub>2</sub>O and Ba<sub>3</sub>Sn<sub>2</sub>O<sub>5</sub>(O<sub>2</sub>)<sub>2</sub>·5H<sub>2</sub>O [9], MgSnO<sub>2</sub>(O<sub>2</sub>)·3H<sub>2</sub>O and Mg<sub>2</sub>SnO<sub>3</sub>(O<sub>2</sub>)·5H<sub>2</sub>O [10], and CaSnO<sub>2</sub>(O<sub>2</sub>)·3H<sub>2</sub>O and Ca<sub>2</sub>SnO<sub>3</sub>(O<sub>2</sub>)·5H<sub>2</sub>O [11].

To prepare stannate powders at the lowest possible temperature, the investigation of the precursor decomposition behaviour is important. The DTA, TG and DTG results for the dried peroxo precursors are illustrated in Fig. 1. A similar degradation behaviour can be observed for the three precursors. There are two stages of weight loss in each case. The precursor powders show an initial weight loss below 300 °C resulting from the evaporation of water. An indication of this process is the endothermic effect in the DTA curves. The decomposition of the peroxide groups occurs in the temperature range between 500 °C and 700 °C. A second endothermic effect in the DTA diagram indicates the release of oxygen. An exotherm above 850 °C observed in all three cases is the result of the crystallization of the strontium stannate phases. The thermal treatment at increasing temperatures is accompanied by a decrease in the specific surface area of the powders. Table II shows the result of BET measurements, including the calculated mean particle sizes for the powders formed during the thermal degradation of the precursor SrSnO<sub>2</sub>(O<sub>2</sub>)·3H<sub>2</sub>O. The specific surface areas with relatively high values correspond with very small particle sizes of the powders. A strong agglomeration, which can be observed in the electron micrographs, is attributed to the high surface energies of the powder particles. Fig. 2 shows the SEM images of the precursor SrSnO<sub>2</sub>(O<sub>2</sub>)·3H<sub>2</sub>O and its decomposition products at 550 °C and 900 °C. A significant grain growth is observed for SrSnO<sub>3</sub> after calcination at 900 °C for 1 h.

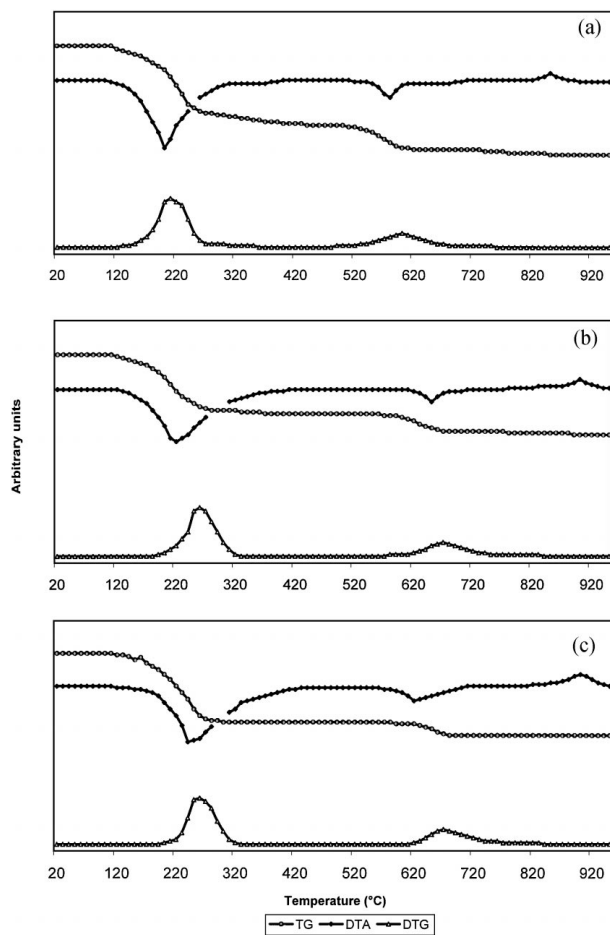
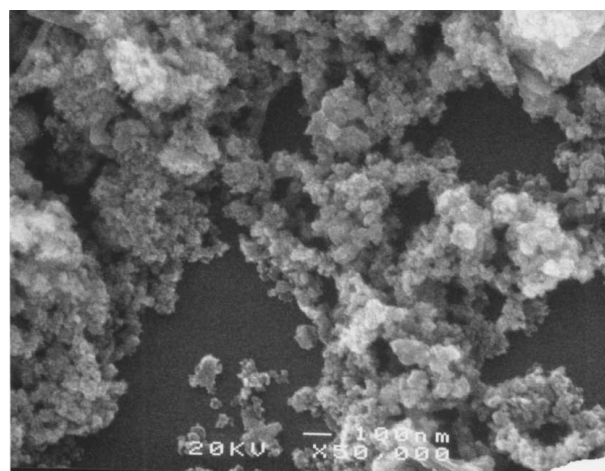


Figure 1 DTA, TG and DTG curves of (a)  $\text{SrSnO}_2(\text{O}_2)\cdot 3\text{H}_2\text{O}$ , (b)  $\text{Sr}_2\text{SnO}_3(\text{O}_2)\cdot 2\text{H}_2\text{O}$  and (c)  $\text{Sr}_3\text{Sn}_2\text{O}_5(\text{O}_2)_2\cdot 5\text{H}_2\text{O}$ .

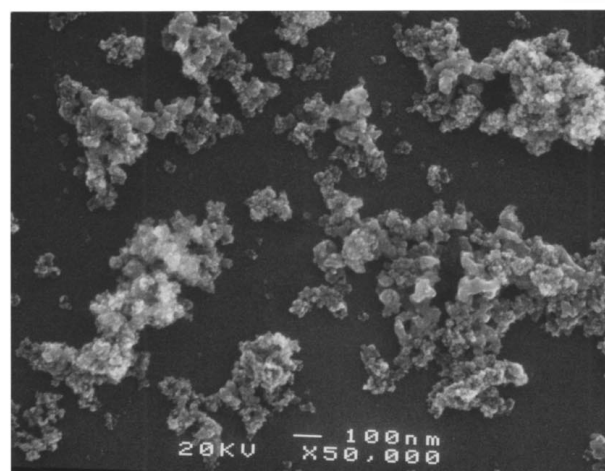
TABLE II Specific surface area and mean particle diameter as a function of the calcination conditions for the powders obtained during  $\text{SrSnO}_3$  formation

Conditions (h/°C) <sup>-1</sup>	Specific surface area (m <sup>2</sup> g <sup>-1</sup> )	Mean particle diameter (μm)
8/200	114	0.01
8/400	90	0.01
8/600	54	0.02
8/800	36	0.03
8/1000	12	0.08

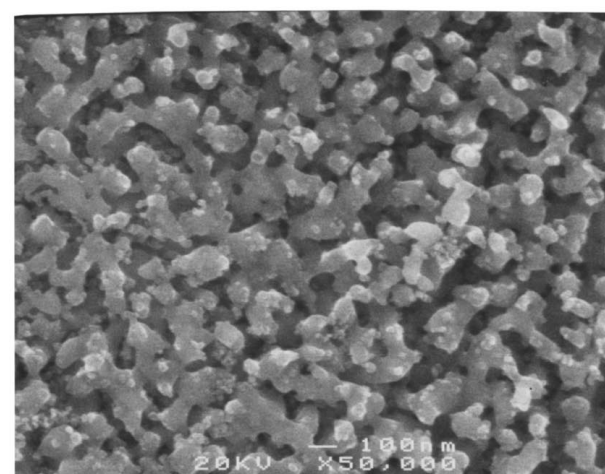
The XRD patterns of the three dried and heat-treated peroxy-precursors are shown in Fig. 3. The diffractograms for samples obtained at temperatures below 500 °C consist of low broad humps indicating X-ray amorphous phases. A comparable situation has been observed for barium, calcium and magnesium stannates formed by thermal degradation of peroxy-precursors [9–11]. The calcination of  $\text{SrSnO}_2(\text{O}_2)\cdot 3\text{H}_2\text{O}$ ,  $\text{Sr}_2\text{SnO}_3(\text{O}_2)\cdot 2\text{H}_2\text{O}$  and  $\text{Sr}_3\text{Sn}_2\text{O}_5(\text{O}_2)_2\cdot 5\text{H}_2\text{O}$  at 550 °C leads to small broad reflections in the diffractograms which indicate the formation of stannate phases,  $\text{SrCO}_3$  and  $\text{SnO}_2$ . There is no evidence for  $\text{SrCO}_3$  and  $\text{SnO}_2$  only in the case of the decomposition of  $\text{SrSnO}_2(\text{O}_2)\cdot 3\text{H}_2\text{O}$ . With increasing temperature above 550 °C, forced crystallization can be observed in all cases. The broad patterns of the powders calcined at



(a)



(b)



(c)

Figure 2 SEM micrographs of (a)  $\text{SrSnO}_2(\text{O}_2)\cdot 3\text{H}_2\text{O}$ , (b) powder obtained after calcination of  $\text{SrSnO}_2(\text{O}_2)\cdot 3\text{H}_2\text{O}$  at 500 °C for 1 h and (c)  $\text{SrSnO}_3$  obtained after calcination of  $\text{SrSnO}_2(\text{O}_2)\cdot 3\text{H}_2\text{O}$  at 900 °C for 1 h.

lower temperatures suggest an incomplete crystallization process.

$\text{SrCO}_3$  and  $\text{SnO}_2$  can be indicated as intermediate phases up to 750 °C during the degradation of  $\text{Sr}_2\text{SnO}_3(\text{O}_2)\cdot 2\text{H}_2\text{O}$  and  $\text{Sr}_3\text{Sn}_2\text{O}_5(\text{O}_2)_2\cdot 5\text{H}_2\text{O}$ . Only stannate phases are found at temperatures above 750 °C. All essential reflections for  $\text{SrSnO}_3$  can be indicated for

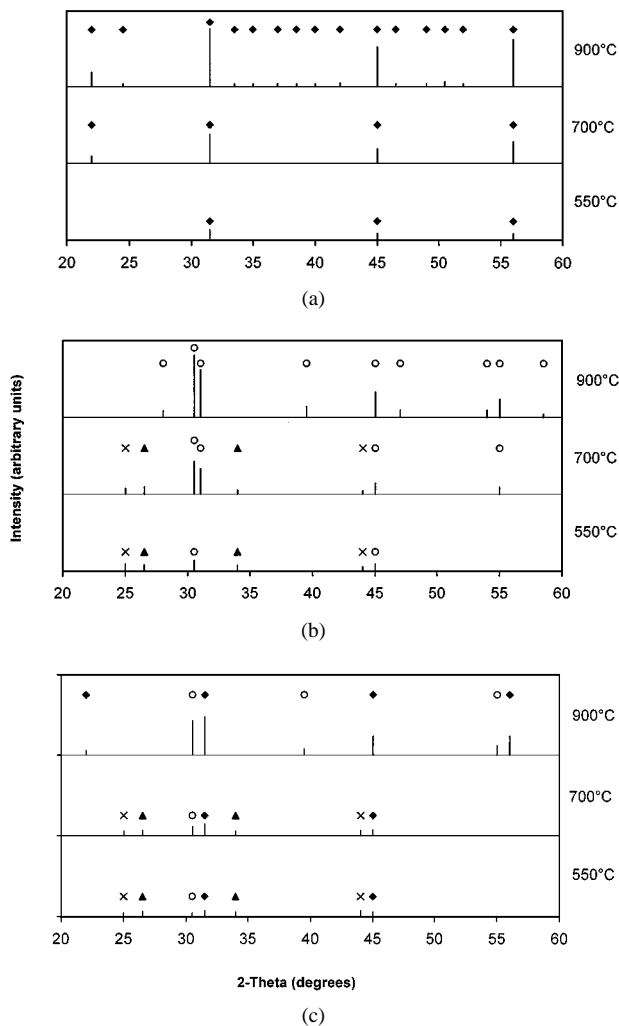


Figure 3 X-ray diffractograms of the decomposition products of (a)  $\text{SrSnO}_2(\text{O}_2)\cdot 3\text{H}_2\text{O}$ , (b)  $\text{Sr}_2\text{SnO}_3(\text{O}_2)\cdot 2\text{H}_2\text{O}$  and (c)  $\text{Sr}_3\text{Sn}_2\text{O}_5(\text{O}_2)_2\cdot 5\text{H}_2\text{O}$  ( $\blacktriangle$   $\text{SnO}_2$ ,  $\times$   $\text{SrCO}_3$ ,  $\blacklozenge$   $\text{SrSnO}_3$ ,  $\circ$   $\text{Sr}_2\text{SnO}_4$ ).

the decomposition of  $\text{SrSnO}_2(\text{O}_2)\cdot 3\text{H}_2\text{O}$  at  $900^\circ\text{C}$ . A comparable situation is observed for the degradation of  $\text{Sr}_2\text{SnO}_3(\text{O}_2)\cdot 2\text{H}_2\text{O}$  at the same temperatures. Only the reflections of  $\text{Sr}_2\text{SnO}_4$  are found in this case in the diffractogram. The reaction of the intermediates  $\text{SrCO}_3$  and  $\text{SnO}_2$  has completed the formation of  $\text{Sr}_2\text{SnO}_4$ .

Another situation has been found for the further decomposition of  $\text{Sr}_3\text{Sn}_2\text{O}_5(\text{O}_2)_2\cdot 5\text{H}_2\text{O}$  above  $750^\circ\text{C}$ . Diffractograms are obtained containing the reflections of  $\text{SrSnO}_3$  as well as  $\text{Sr}_2\text{SnO}_4$ . Both stannates seem to be formed in an equimolar ratio. There is no evidence for the formation of a stannate  $\text{Sr}_3\text{Sn}_2\text{O}_7$ . At  $1200^\circ\text{C}$ , very sharp peaks corresponding exactly to the patterns of  $\text{SrSnO}_3$  and  $\text{Sr}_2\text{SnO}_4$  are observed. The precursor  $\text{Ba}_3\text{Sn}_2\text{O}_5(\text{O}_2)_2\cdot 5\text{H}_2\text{O}$  decomposes in a similar manner to  $\text{BaSnO}_3$  and  $\text{Ba}_2\text{SnO}_4$  [9].  $\text{Ba}_3\text{Sn}_2\text{O}_7$  could not be formed by this route, too.

Fig. 4 shows the densification curves for  $\text{SrSnO}_3$  and  $\text{Sr}_2\text{SnO}_4$  compacts obtained by isothermal sintering at  $1200^\circ\text{C}$  and  $1400^\circ\text{C}$ . Table III contains the results of surface area measurements and analytical investigations for the  $\text{SrSnO}_3$  and  $\text{Sr}_2\text{SnO}_4$  powders applied for the sintering experiments. Only relatively small amounts of impurities are indicated by the quantitative analysis. Carbonate was not detected in any case. The

TABLE III Specific surface area and analytical data of the powders used for the sintering experiments

Powder	Specific surface area ( $\text{m}^2 \text{g}^{-1}$ )	$D_{\text{BET}}$ ( $\mu\text{m}$ )	Impurities (ppm)				
			Al	Ba	Na	Si	Ca
$\text{SrSnO}_3$	15	0.06	60	30	90	10	60
$\text{Sr}_2\text{SnO}_4$	14	0.07	70	40	80	20	70

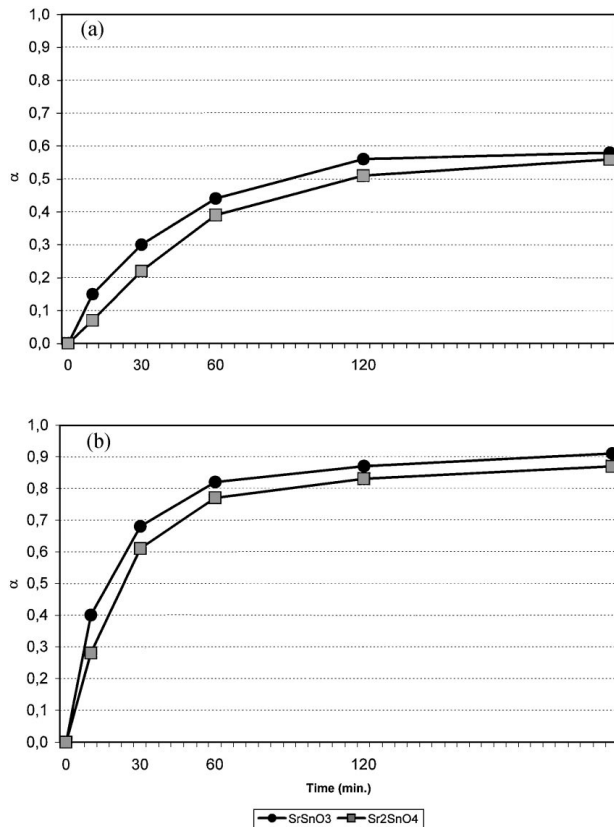


Figure 4 Densification parameter of  $\text{SrSnO}_3$  and  $\text{Sr}_2\text{SnO}_4$  compacts as a function of isothermal heating time at (a)  $1200^\circ\text{C}$  and (b)  $1400^\circ\text{C}$ .

purity of the strontium stannates prepared using the peroxide route is significantly better than that of comparable powders with the same composition synthesized by the solid state reaction between  $\text{SrCO}_3$  and  $\text{SnO}_2$ . The higher purity together with the more advantageous morphologic situation can be the basis of better properties of functional electronic elements produced using the peroxide derived stannate powders.

The densification parameter  $\alpha$  is calculated with the relation  $\alpha = (\rho_t - \rho_0) / (\rho_{\text{th}} - \rho_0)$ , where  $\rho_0$  is the starting density after compacting,  $\rho_t$  is the density at a given time, and  $\rho_{\text{th}}$  is the theoretical density ( $6.43 \text{ g cm}^{-3}$  for  $\text{SrSnO}_3$ ,  $5.78 \text{ g cm}^{-3}$  for  $\text{Sr}_2\text{SnO}_4$ ). The equation has regard to the different starting densities in a favourable manner. The  $\rho_0$  values are  $3.01 \text{ g cm}^{-3}$  for  $\text{SrSnO}_3$  (47% of  $\rho_{\text{th}}$ ) and  $2.92 \text{ g cm}^{-3}$  for  $\text{Sr}_2\text{SnO}_4$  (51%) compacts. Sintering at  $1200^\circ\text{C}$  leads in both cases to a remarkable shrinkage of the stannate samples. The densification is slightly better for  $\text{SrSnO}_3$  compared with  $\text{Sr}_2\text{SnO}_4$ . The highest densities after 4 h at  $1200^\circ\text{C}$  are  $5.03 \text{ g cm}^{-3}$  for  $\text{SrSnO}_3$  (78%) and  $4.52 \text{ g cm}^{-3}$  for  $\text{Sr}_2\text{SnO}_4$  (78%). Sintering at  $1400^\circ\text{C}$  leads to extremely strong densification of the compacts. Densities near to the theoretical

values are obtained. The highest densities measured after 4 h at 1400 °C are 6.11 g cm<sup>-3</sup> for SrSnO<sub>3</sub> (95%) and 5.38 g cm<sup>-3</sup> for Sr<sub>2</sub>SnO<sub>4</sub> (93%). Comparable sintering studies with strontium stannates formed via the solid state reaction show significantly worse sinterability. The obtained densities have values of about 90% of  $\rho_{th}$ . The densities obtained after sintering of barium, magnesium and calcium stannates formed via the peroxide route are comparable with those of the here described strontium stannates SrSnO<sub>3</sub> and Sr<sub>2</sub>SnO<sub>4</sub> [9–11]. The highest density has been measured for CaSnO<sub>3</sub> after sintering at 1400 °C with 97% of  $\rho_{th}$  [11].

#### 4. Conclusions

A successful low-temperature process has been developed to synthesize very fine SrSnO<sub>3</sub> and Sr<sub>2</sub>SnO<sub>4</sub> powders. Peroxo precursors result from reactions of strontium- and tin-containing solutions with hydrogen peroxide and ammonia. The obtained precursors are amorphous but show definite stoichiometries. Their thermal treatment at temperatures above 900 °C leads to single-phase crystalline stannates at lower temperatures than in the case of using the conventional solid state reaction. The thermal degradation leads directly to the stannate in the case of SrSnO<sub>3</sub>. SrCO<sub>3</sub> and SnO<sub>2</sub> occur as intermediates during the formation of Sr<sub>2</sub>SnO<sub>4</sub>

starting from the precursor Sr<sub>2</sub>SnO<sub>3</sub>(O<sub>2</sub>)·2H<sub>2</sub>O. Experiments to synthesize the composition Sr<sub>3</sub>Sn<sub>2</sub>O<sub>7</sub> lead to negative results. A stoichiometric precursor is formed also in this case, but the thermal decomposition at higher temperatures yields a mixture of SrSnO<sub>3</sub> and Sr<sub>2</sub>SnO<sub>4</sub> in the ratio 1 : 1.

#### References

1. W. W. COFFEEN, *J. Amer. Ceram. Soc.* **36** (1953) 207.
2. Y. SHIMIZU, M. SHIMALUKURO, H. ARAI and T. SEIYAMA, *J. Electrochem. Soc.* **136** (1989) 1206.
3. R. WERNICKE, *Ber. Dtsch. Keram. Ges.* **55** (1978) 356.
4. W. PUKALL, *Silikat-Z.* **2** (1914) 65.
5. A. HOFFMANN, *Z. Phys. Chem.* **B28** (1935) 65.
6. P. APPENDINO and G. RAMONDA, *Ann. Chim. (Rome)* **60** (1970) 407.
7. A. VEGAS, *Acta Crystallogr.* **B42** (1986) 167.
8. R. WEISS and R. FAIVRE, *C. R. Acad. Sci.* **248** (1959) 106.
9. G. PFAFF, *J. Eur. Ceram. Soc.* **12** (1993) 159.
10. *Idem.*, *Thermochim. Acta* **237** (1994) 83.
11. *Idem.*, *Mater. Sci. Eng.* **B33** (1995) 156.
12. *Idem.*, *J. Mater. Sci.* **27** (1992) 1222.
13. *Idem.*, *J. Eur. Ceram. Soc.* **9** (1992) 121.
14. *Idem.*, *ibid.* **9** (1992) 293.
15. *Idem.*, *Ceram. Int.* **20** (1994) 111.
16. *Idem.*, *Mater. Lett.* **24** (1995) 393.

*Received 27 April  
and accepted 10 December 1999*